NINETEENTH EUROPEAN ROTORCRAFT FORUM

Paper n° C12

# COMPARISON BETWEEN FP3D FULL POTENTIAL CALCULATIONS AND S1 MODANE WIND TUNNEL TEST RESULTS ON ADVANCED FULLY INSTRUMENTED ROTORS

by

P. BEAUMIER, M. COSTES, R. GAVERIAUX

ONERA, FRANCE

September 14–16, 1993
CERNOBBIO (Como)
ITALY

ASSOCIAZIONE INDUSTRIE AEROSPAZIALI
ASSOCIAZIONE ITALIANA DI AERONAUTICA ED ASTRONAUTICA

# Comparison between FP3D Full Potential Calculations and S1 Modane wind tunnel test results on advanced fully instrumented rotors *

P. Beaumier, M. Costes, R. Gaveriaux, ONERA

* ( This work received financial support from French ministry of defense : DRET , STPA )

**Abstract**

A comparison is made between FP3D Full Potential calculations and S1 Modane wind tunnel test results. A short description of the wind tunnel tests and of the computational methods used is first given. The influence of advance ratio and rotational speed, as well as that of the blade tip geometry are shown and compared to experiment. Correlations are generally of good quality but refinements are proposed in order to improve the calculations. Nevertheless the results given in the paper show that the present CFD method has reached a point where it can be very helpful in the design process.

## 1 INTRODUCTION

Computer codes are now widely used to solve dynamic and aerodynamic problems occuring on helicopter rotor blades. A first group of such methods combine very simple aerodynamic models (eg. lifting line) with 'complete' dynamic and elastic blade models to trim the rotor. These methods are fast and widely used by helicopters manufacturers for design.

However the limits of such codes are quickly reached in high speed flight conditions, where compressibility effects occur or for non rectangular blade geometries. These effects are then modelled by semi-empirical formula and partially included in 2D airfoil tables. CFD methods, which solve the numerical flow field equations around the blade, are capable of simulating these effects. Computer codes solving potential equations or Euler equations are more and more used for research purposes [1]. However, since they are very CPU time consuming they cannot be easily coupled with blade dynamics equations and therefore need external trim conditions given by the simpler methods mentioned above.

In parallel to the use of computer codes, manufacturers and research

centers make a constant effort on wind tunnel or flight tests : these are very important to validate new computational concepts and methods, which invariably have to make simplifying assumptions.

In this paper, a comparison is made between FP3D Full Potential calculations and S1 Modane wind tunnel test results. Wind tunnel tests are described in the 1st part of the paper. The 2nd part of it is devoted to a brief description of the computational methods. The influence of advance ratio and rotational speed are then commented showing the capabilities and limits of the present CFD method. Some improvements are then proposed before drawing some conclusions on the ability of this method to represent real physical phenomena and to be used in the design process.

## 2 S1 MODANE WIND TUNNEL TESTS

Two fully instrumented rotors were tested in 1991 in the ONERA S1 wind tunnel at Modane test center [2]. They are the 7A and the 7AD rotors which are modern rotors designed by Eurocopter France (ECF) and only differ by their blade tip shape : the 7A rotor has rectangular blades while the 7AD rotor has a SPP8 parabolic tip with taper, sweep and anhedral (fig. 1). Both rotors have OA213 airfoil (13% relative thickness) from blade root to 75% radius and OA209 airfoils (9% relative thickness) from 90% radius to blade tip. The 7A and 7AD rotors have the same geometric twist (fig. 2) corresponding to a linear aerodynamic twist of −3.95 °/m, and both rotors have an aspect ratio equal to 15.

The rotor instrumentation includes 116 unsteady pressure transducers distributed on 5 sections (r/R=0.5, 0.7, 0.825, 0.915 and 0.975) and 30 strain gauges regularly distributed all along the blade to compute blades deformation using Strain Pattern Analysis [3].

The test envelope covers advance ratios from 0.3 to 0.5, a thrust coefficient $C_T/\sigma$ from 0.05 to 0.10 and a non dimensional propulsive force $(C_dS)/S\sigma$ from 0.07 to 0.15. Three rotating tip Mach numbers were investigated ($M_{\Omega R}$=0.617, 0.646 and 0.676) for the same flight conditions and for both rotors.

For all test conditions presented in this paper, the rotor was trimmed according to the so called 'Modane law' : $\beta_{1c} = -\theta_{1s}$, $\beta_{1s} = 0$.

## 3 COMPUTATIONAL METHOD

This extensive database is particularly suited to CFD codes validation. The ONERA Unsteady Full Potential code FP3D ([4], [5]) was used to compute a wide range of wind tunnel test conditions described above. This method is

capable of computing the non linear unsteady flows around an isolated blade. Mass conservation (1) and Bernoulli (2) equations are solved in a rotating frame (fig. 3).

$$\partial_t(\frac{\rho}{J}) + \partial_\xi(\frac{\rho U}{J}) + \partial_\eta(\frac{\rho V}{J}) + \partial_\zeta(\frac{\rho W}{J}) = 0 \qquad (1)$$

$$\rho = \{ 1 + \frac{\gamma-1}{2}( -2.\phi_t - (U+\xi_t).\phi_\xi - (V+\eta_t).\phi_\eta - (W+\zeta_t).\phi_\zeta ) \}^{\frac{1}{\gamma-1}} \qquad (2)$$

Boundary conditions used are the following :

- blade surface : a 'transpiration condition' is used to simulate both the influence of the other blades and the full rotor wake, and to take into account the blade dynamics.
- wake : a potential discontinuity $\Gamma$ through a virtual surface issued from the trailing edge of the blade is imposed for 'lifting' configurations. A convection equation is solved because the circulation $\Gamma$ is time dependant for unsteady computations.
- inboard section : the transverse potential velocity due to the blade is assumed to be equal to zero.
- grid boundaries : non reflecting boundary conditions are used, given by a linearized wave equation solved at the mesh boundaries.

An implicit time dependent equation for the potential is obtained from density and flux linearizations. This equation is solved using a finite difference method with $2^{nd}$ order spatial centered derivatives and $1^{st}$ order time derivatives.

For supersonic flows a flux biasing density upwinding is introduced using an Engquist–Osher formulation.

The computational domain consists of a C mesh from 0.5 to 1.6 times blade radius and covers an angular sector of 6 chords at blade tip.

Partial inflow angles are computed by R85/METAR code [6]. This rotor performance code, initially developed at ECF, uses a lifting line analysis with a vortex wake of prescribed geometry. At each blade section and for a given azimuth, the influence of all the vortex lattices located outside the computational domain are computed. The influence of lattices inside the computational domain and coming directly from the computed blade is excluded because it is already part of the FP3D solution.

Finally, the partial inflow angles also take into account blade dynamics.

# 4 COMPARISONS BETWEEN COMPUTATIONS AND EXPERIMENT

## 4.1 Influence of advance ratio and rotational speed

Influence of advance ratio

Four calculations were performed to study the influence of advance ratio on the 7A rotor : $\mu$=0.3, 0.4, 0.45 and 0.5. These computations were carried out under the following conditions : $M_{\Omega R}$=0.646, Cl/$\sigma$=0.075 and (CdS)/S$\sigma$=0.1

For the lowest advance ratio ($\mu$=0.3), the pressure distribution on the advancing side is fairly well predicted (fig. 4). Near $\psi$=180°, results are still good (fig. 5). On the retreating side, the correlation is less satisfactory for r/R=0.5, where the flow cannot be assumed to be inviscid (fig. 6).

For high advance ratios ($\mu$=0.45 or 0.5), computations are still of good quality on the advancing side, but the extension of the supersonic zone after $\psi$=90° is over–estimated (fig. 7). More precisely, the experimental shock location is closer to the leading edge than in the calculations. This can be attributed to the inviscid and isentropic assumptions which are probably not correct for such severe conditions ($\mu$=0.5). Another reason for this can come from the incidences given by R85/METAR, and more particularly from the prediction of torsional deformations. The way these deformations are taken into account in FP3D (transpiration condition) can also be criticized : the real unsteady pitching motion of the blade is yet not modelled in FP3D.

Figure 8 illustrates the extension of supersonic zones when advance ratio increases. At $\psi$=90°, we can notice on figure 9 that the supersonic zone on the blade is connected to the supersonic zone outside the blade in the rotating frame for high advance ratios (delocalization effect penalyzing for impulsive noise).

Influence of rotational speed

In this section, the following conditions were chosen : 7AD rotor, Cl/$\sigma$*=0.0625, (CdS)/S$\sigma$*=0.1 and $\mu$*=0.45. Three different tip Mach numbers were investigated : $M_{\Omega R}$=0.617, 0.646 and 0.676.

Note that these three cases correspond to the same flight conditions because the non dimensional coefficients Cl/$\sigma$*, (CdS)/S$\sigma$* and $\mu$* were referenced to the same velocity ( ~ 220 m/s).

On the advancing side, increasing the rotating tip Mach number tends to increase shock intensity at the blade tip, as could be expected. This trend is quantitatively well predicted by the computations (fig. 10). This also explains the increase of drag and torque coefficients when $M_{\Omega R}$ increases.

On the front side and the retreating side of the rotor disk, configurations with a lower tip Mach number are more loaded because incidences need to be higher to produce the same total lift (fig. 11a and 11b).

## 4.2 Comparison between 7A and 7AD rotors

In this section, the pressure distributions for rotors 7A and 7AD are compared for $M_{\Omega R}$=0.646, $\mu$=0.4 and Cl/$\sigma$=0.075.

From the experimental point of view, figure 12 shows that these pressure distributions are very similar up to r/R=0.700 and differences become more important at r/R=0.975, where the blade geometries are different. A decrease in shock intensity on the 7AD blade is found.

Computations simulate this effect correctly (fig. 13) : there is an important decrease in the extension of the supersonic zone on the 7AD blade. Consequently, the 7AD rotor requires less power than the 7A rotor in this configuration.

## 4.3 Influence of wind tunnel corrections

All the computations presented above assume that the flow coming to the rotor is perfectly uniform. Unfortunately, this is not the case in wind tunnels because of wind tunnel walls and rotor test rig deflections. In the case of S1 Modane, a correction procedure was developped to take these effects into account. It uses a panel method simulation to compute additional induced velocities at the rotor disk to be introduced into R85/METAR. This study showed that these deflections are particularly large for low shaft angles $\alpha_q$ and that comparisons between calculations and experiment could be significantly improved by introducing these corrections in the rotor simulation. More precisely, it was found that torque coefficient, lateral pitch coefficient $\theta_{1c}$ and even lift distribution were better predicted.

Consequently, a new FP3D computation was run using the new inflow coming from R85/METAR calculations with wind tunnel geometry corrections. This calculation was done on the 7A rotor for $\mu$=0.3 (a configuration with a low shaft angle).

As illustrated in fig. 14, the new computation shows a slight increase of lift in the front part of rotor disk ($\psi$=180°) and the lift decreases near azimuth $\psi$=360°, for the sections located near the rotor shaft (r/R=0.5). Moreover, a better comparison with experiment can be seen on the advancing side at the blade tip were the shock intensity and location is better predicted with the corrections (fig. 15).

Therefore the wind tunnel corrections have improved the correlations for this 'low speed' case. Another computation was run at higher speed : the benefits brought by the correction procedure are smaller because the shaft angle $\alpha_q$ is higher.

# 5 CONCLUSIONS

The high quality data obtained in the S1 Modane wind tunnel was used to extensively validate the unsteady Full Potential code FP3D in high speed forward flight conditions. The wind tunnel models are two fully instrumented modern rotors designed by ECF, the 7A and 7AD rotors which only differ by their blade tip (rectangular versus SPP8 tip).

The influence of rotor tip speed, advance ratio and blade tip geometry were more particularly investigated. For one configuration, the influence of wind tunnel corrections was also added. The results generally show good agreement between computation and experiment, and the calculated influence of the parameters mentioned above is also well predicted. However, the transonic flows are generally overestimated by the calculations, especially when strong shocks occur.

These differences could be expected from an inviscid potential calculation and in future, new calculations will be carried out with a refined model, including entropy and boundary layer corrections. An improved way of taking into account the blade flexibility (especially torsional deformations) will also be introduced by a real coupling between the blade aerodynamics and dynamics. Nevertheless, this validation work shows that FP3D coupled with R85/METAR can already be used as an efficient tool for modern blade design.

# 6 REFERENCES


[1] M. Costes, R. Houwink, A. Kokkalis, K. Pahlke, A. Saporiti, Application of European CFD methods for helicopter rotors in forward flight, 18th European Rotorcraft Forum, Avignon, Sept. 1992

[2] C. Polacsek, P. Lafon, High Speed Impulsive noise and aerodynamic results for rectangular and swept blade tip in S1 Modane wind tunnel, 17th European Rotorcraft Forum,Berlin, Sept. 1991

[3] N. Tourjansky, E. Szechenyi, The measurement of blade deflections, 18th European Rotorcraft Forum, Avignon, Sept. 1992

[4] M. Costes, A. Desopper, P. Ceroni, P. Lafon, Flow field prediction for helicopter rotor with advanced blade tip shapes using CFD techniques, 2nd int. conf. on basic Rotorcraft Research, College Park (Univ. of Maryland), Fev. 1988

[5] H. Bezard, M. Costes, An improved method for the computation of unsteady transonic potential flow. Application for airfoil and blade performance prediction, 15th European Rotorcraft Forum, Amsterdam, Sept. 1989

[6] G. Arnaud, P. Beaumier, Validation of R85/METAR on the Puma RAE flight tests, 18th European Rotorcraft Forum, Avignon, Sept. 1992

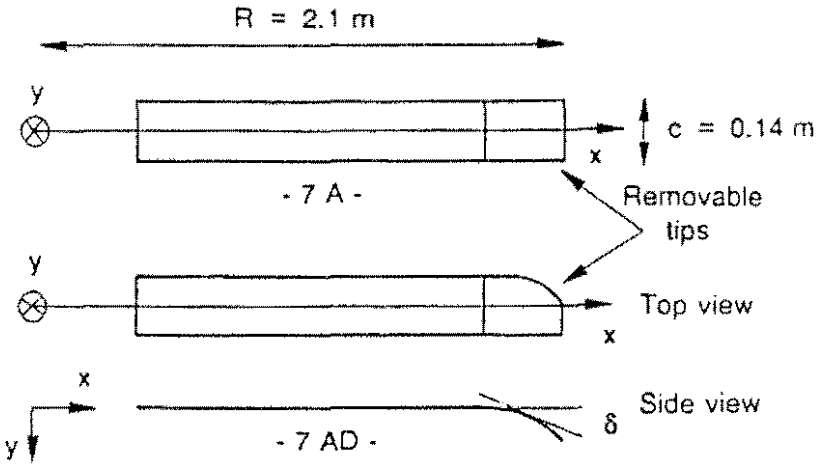


Fig.1 : GEOMETRIC DEFINITION OF 7A AND 7AD ROTORS

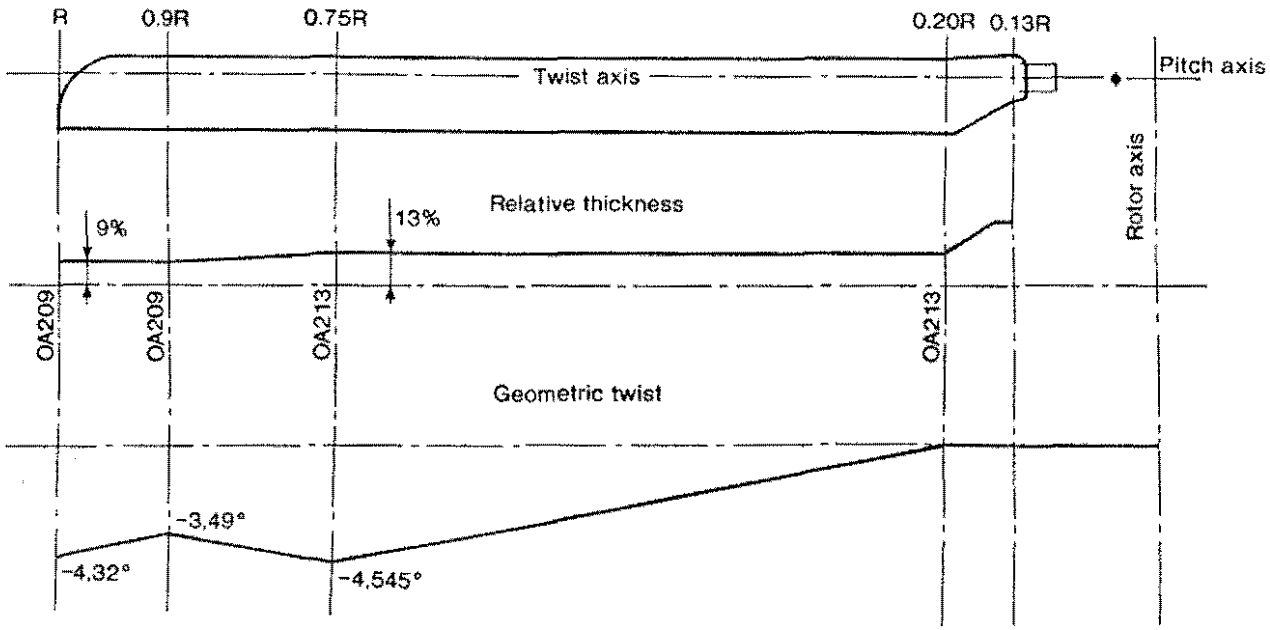


Fig.2 : AERODYNAMIC DEFINITION OF 7A AND 7AD ROTORS

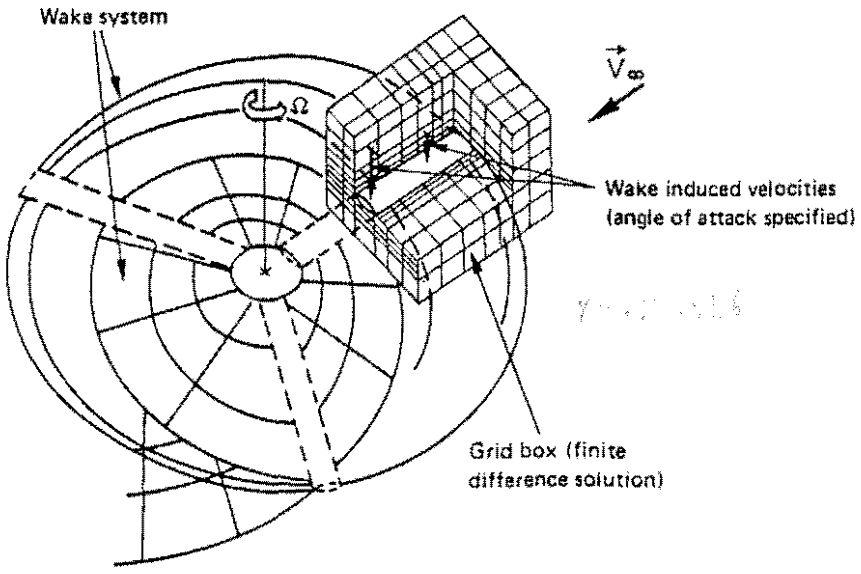


Fig.3 : FP3D WAKE MODELING

PRESSURE DISTRIBUTION ON THE 7A BLADE FOR μ=0.30

- - - - FP3D computation  + Experiment upper surface  * Experiment lower surface

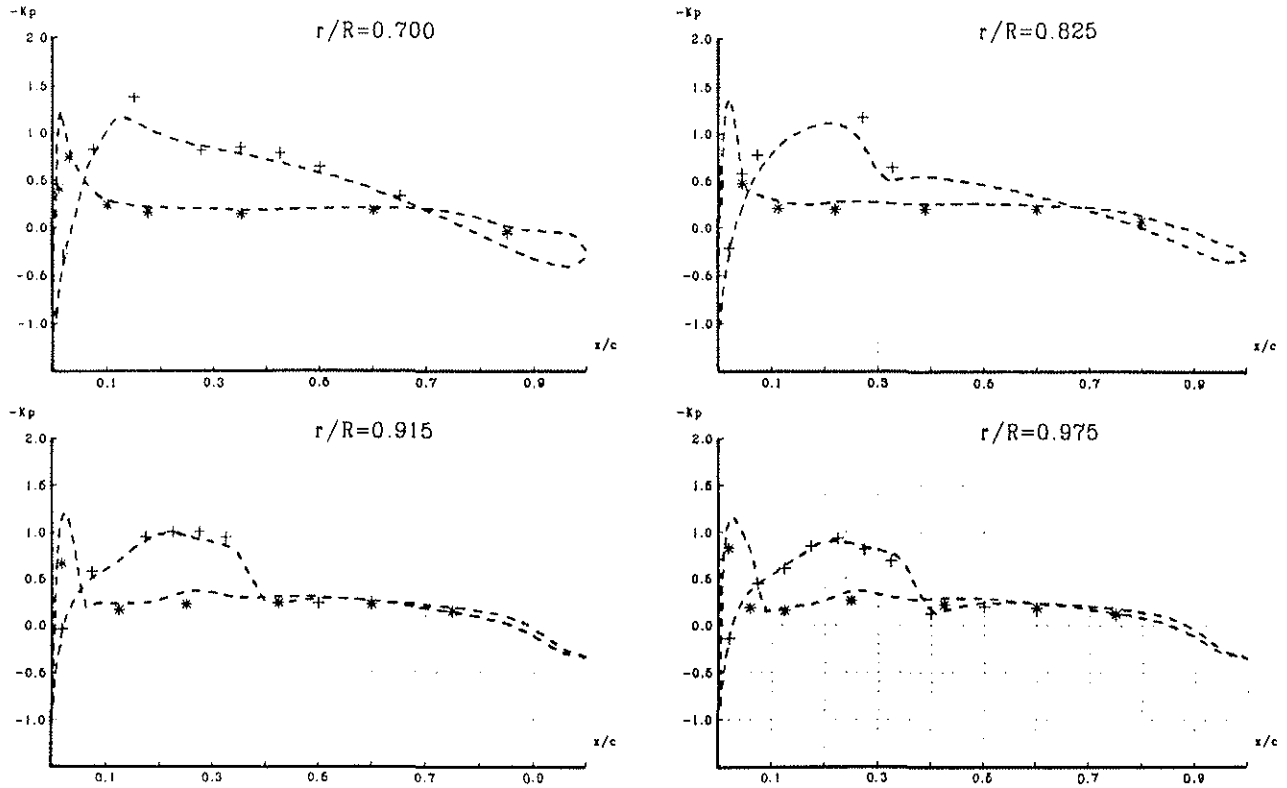


Fig.4 : ψ=90°

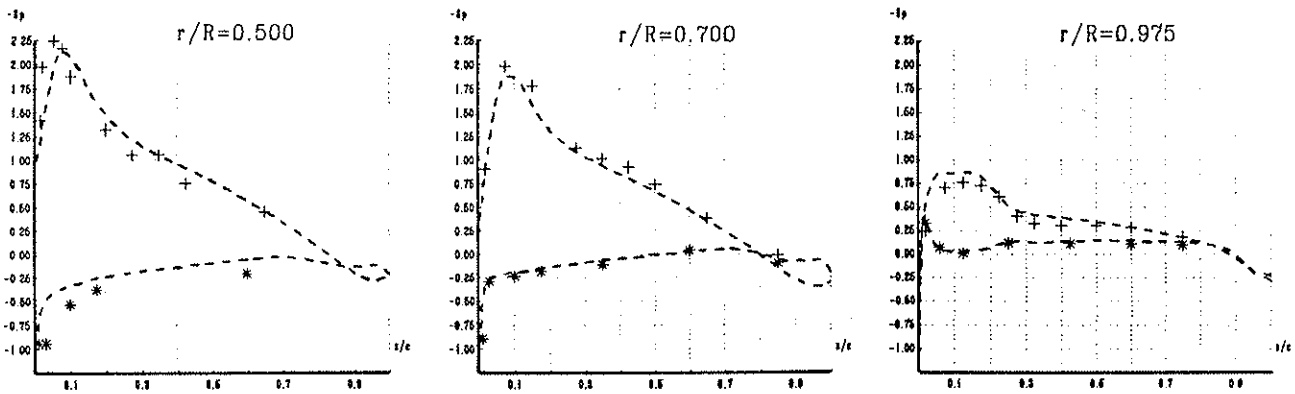


Fig.5 : ψ=180°

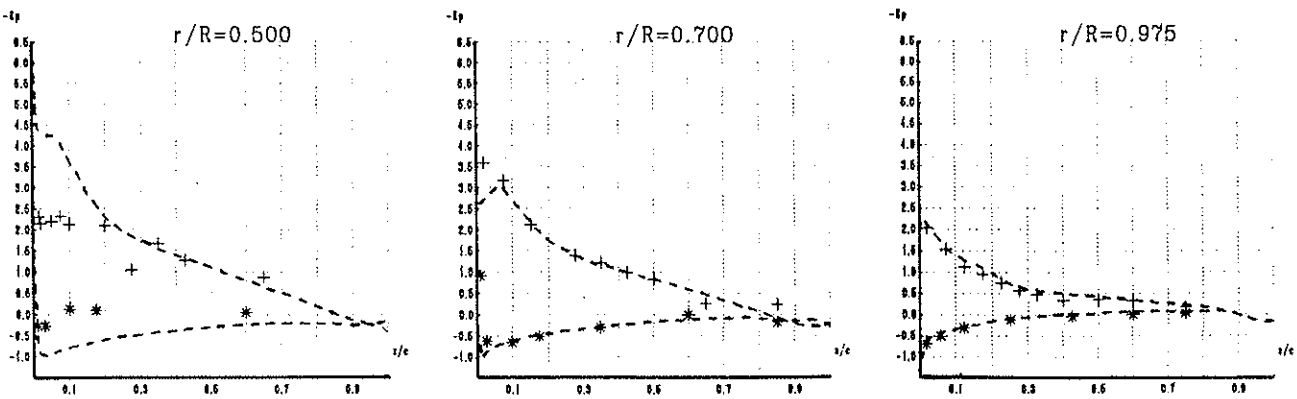


Fig.6 : ψ=270°

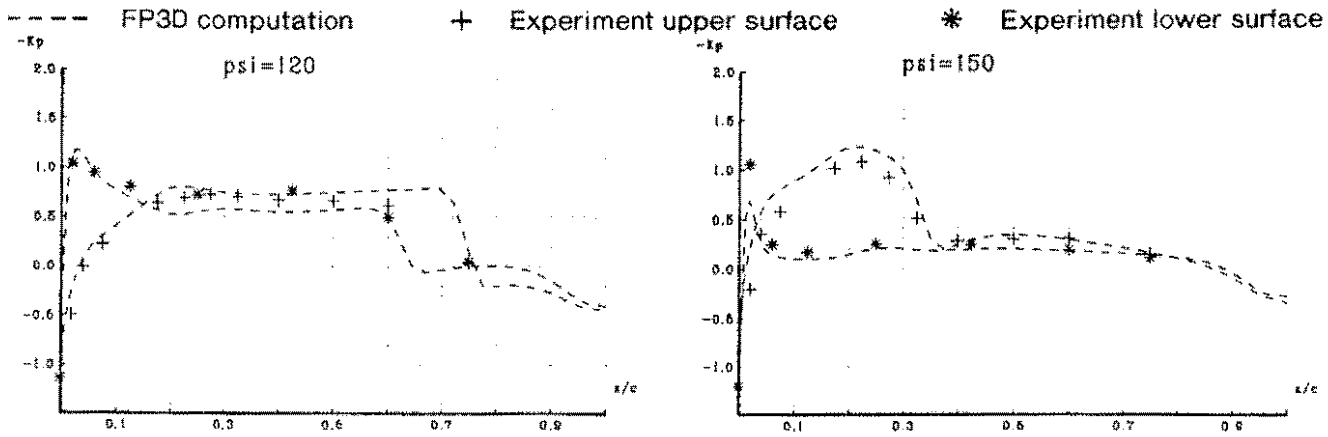


Fig.7 : PRESSURE DISTRIBUTION ON THE 7A BLADE FOR μ=0.45 (r/R=0.915)

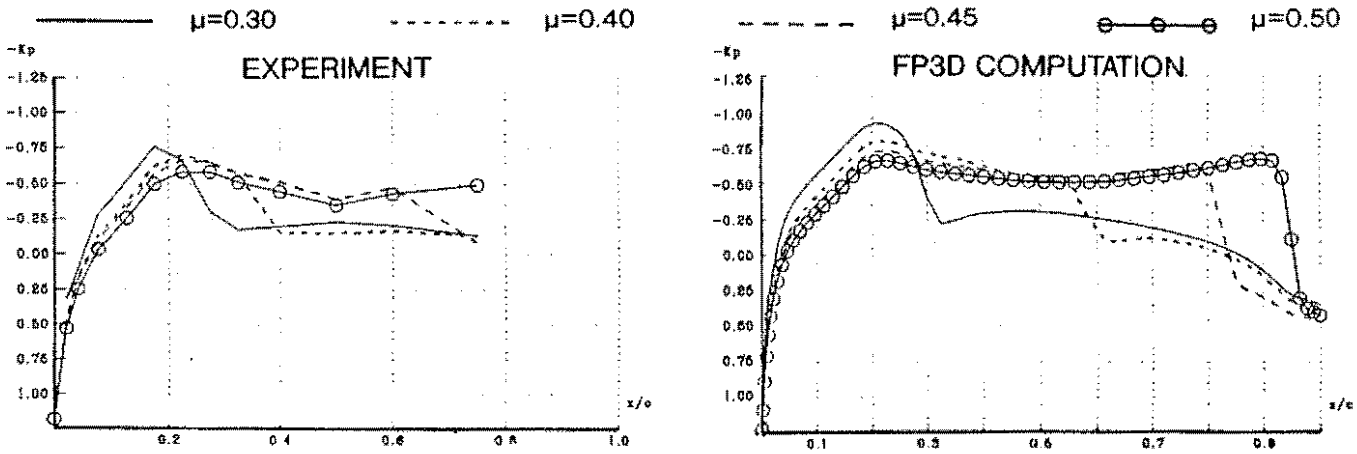


Fig.8 : INFLUENCE OF ADVANCE RATIO ON UPPER SURFACE r/R=0.975 ψ=120°

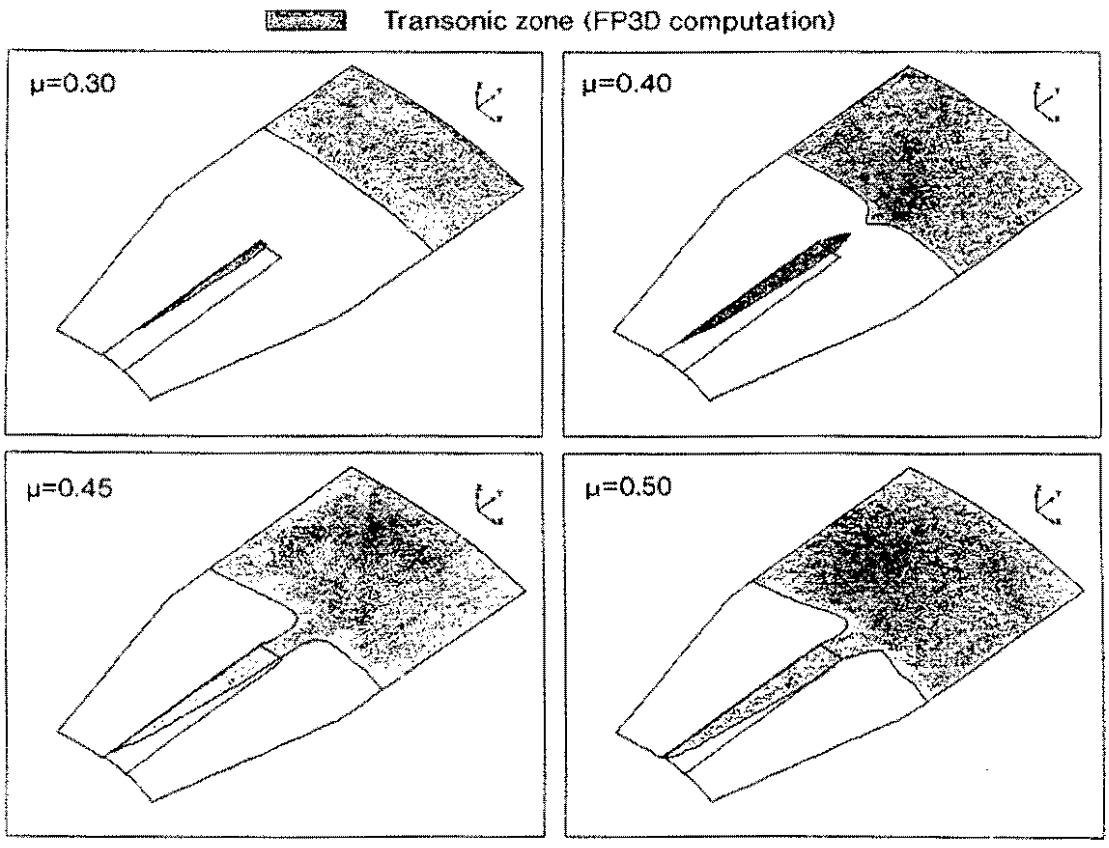


Fig.9 : EVOLUTION OF TRANSONIC ZONE WITH ADVANCE RATIO ON UPPER SURFACE (ψ=90°)

INFLUENCE OF ROTATIONAL SPEED ON 7AD ROTOR $\mu^*=0.45$ $C\ell/\sigma^*=0.0625$

——— MΩR=0.617 – – – – – MΩR=0.676

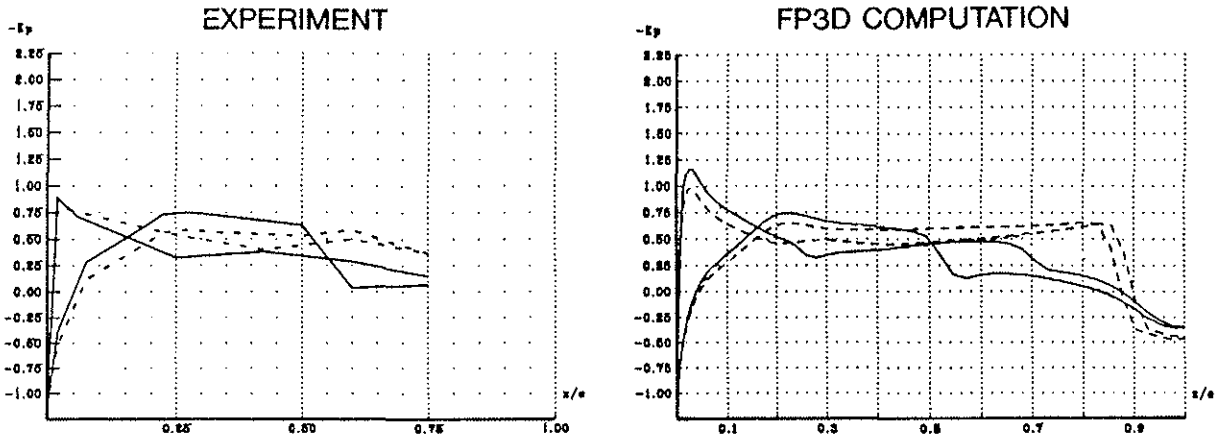


Fig.10 : ψ=90° , r/R=0.915

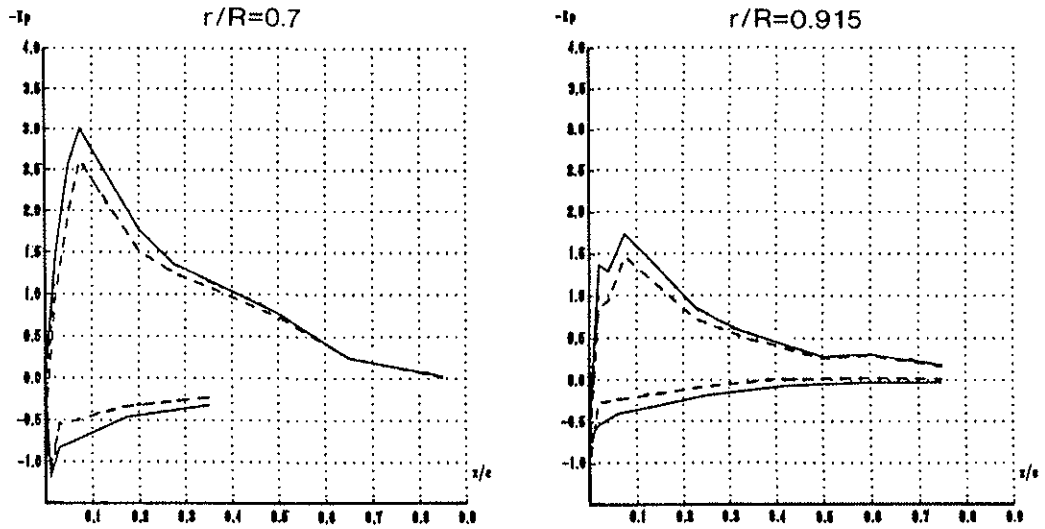


Fig.11a : EXPERIMENT , ψ=180°

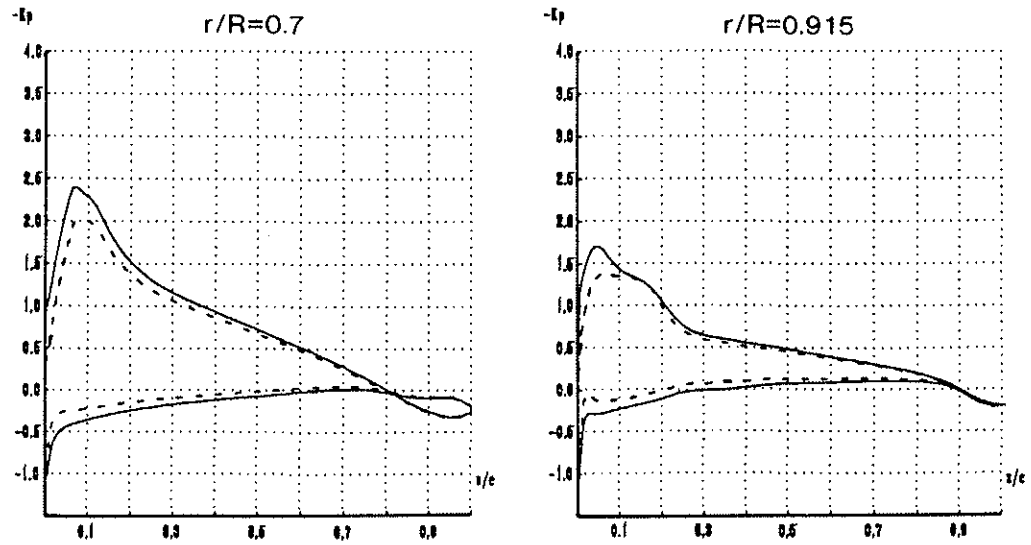


Fig.11b : FP3D COMPUTATION , ψ 180°

COMPARISON BETWEEN 7A AND 7AD ROTORS $\mu = 0.4$ $M\Omega R = 0.646$ $C\ell/\sigma = 0.075$ $\psi = 90°$

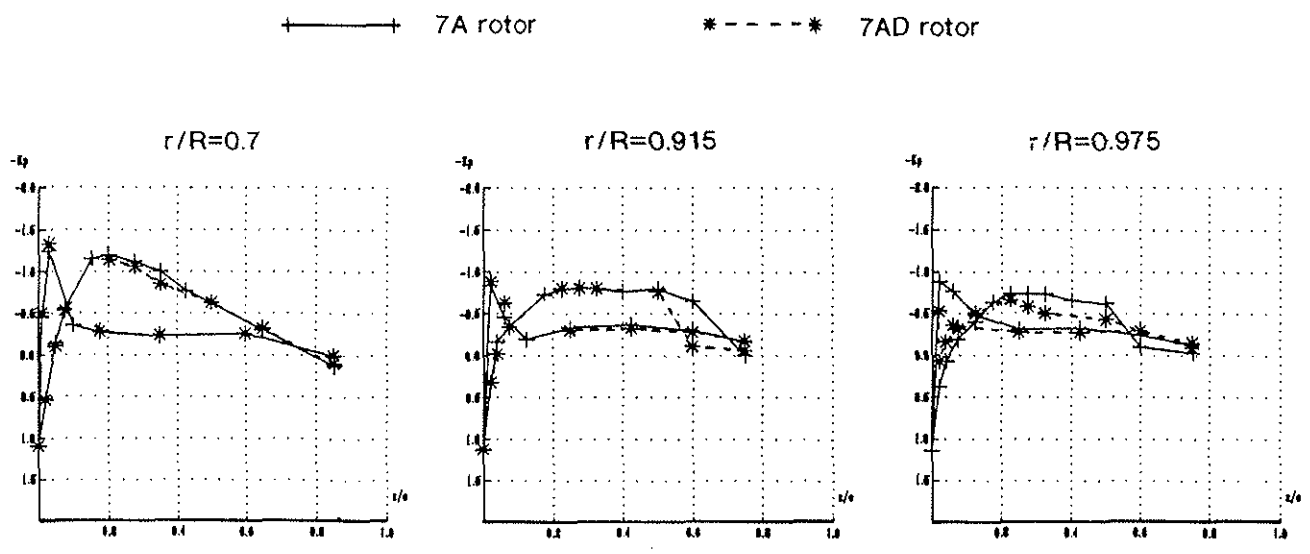


Fig.12 : EXPERIMENT

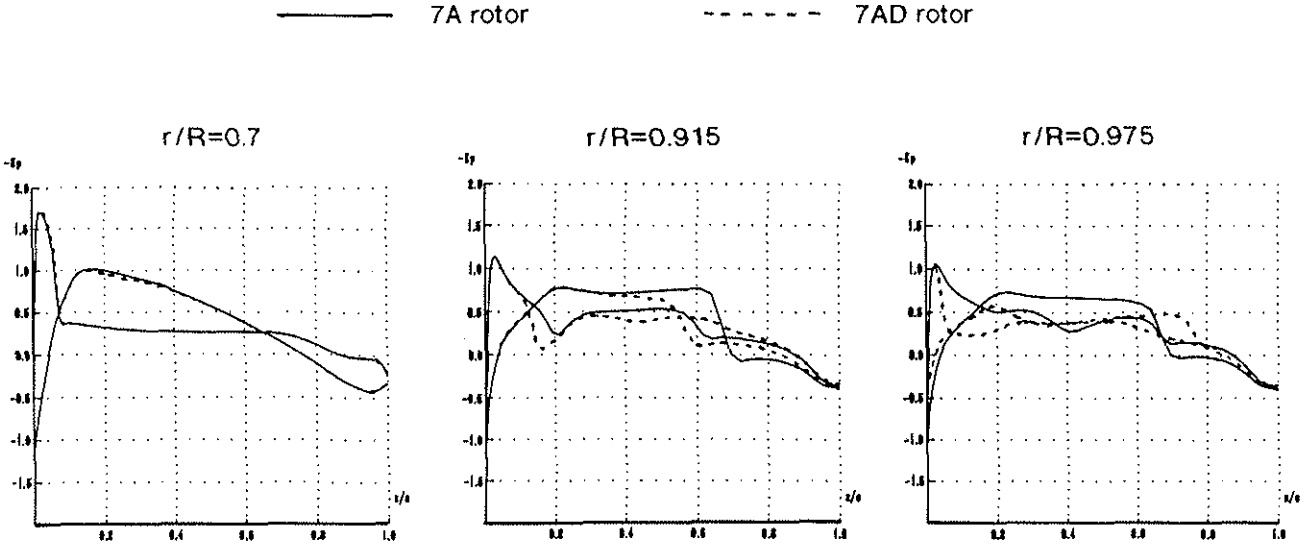


Fig.13 : FP3D COMPUTATION

## INFLUENCE OF WIND TUNNEL CORRECTIONS

——— FP3D Computation
- - - - - FP3D Computation with wind tunnel corrections
+ + + Experiment lower surface
× × × Experiment upper surface

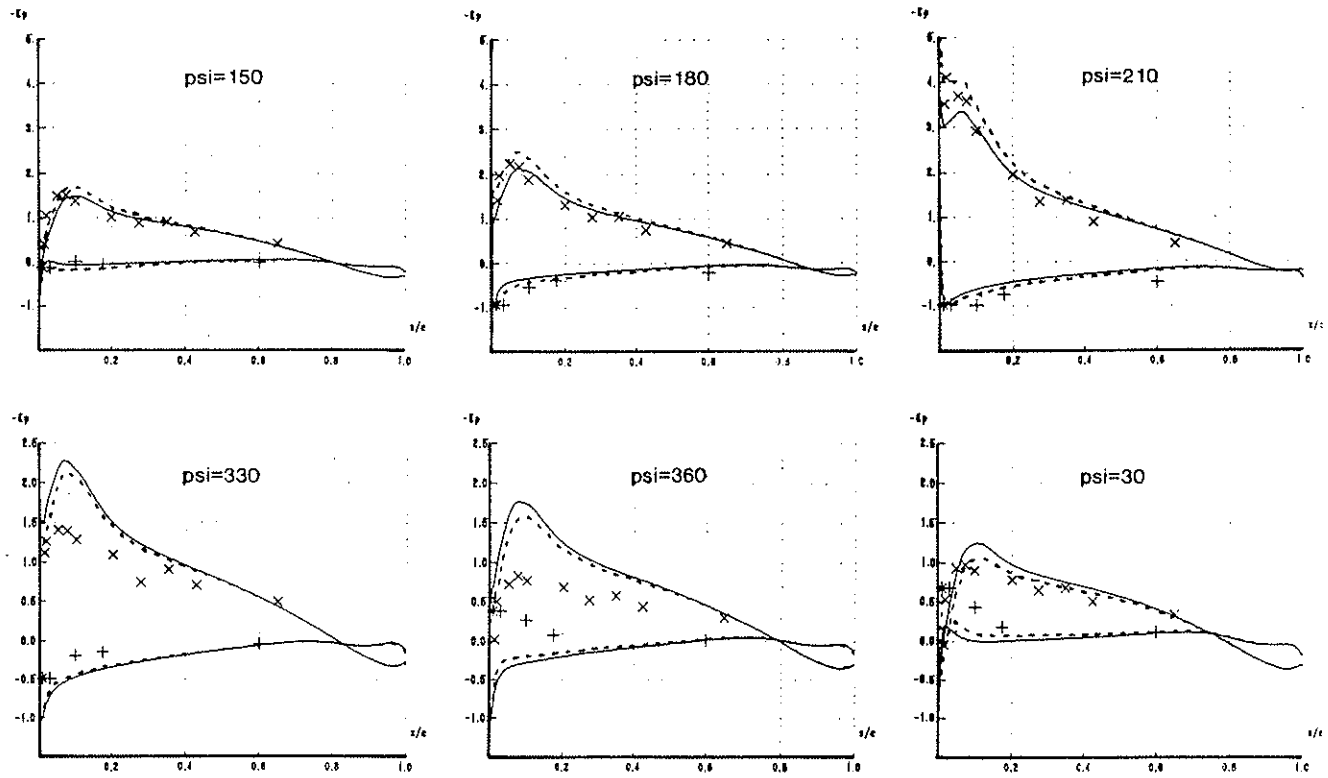


Fig.14 : r/R = 0.5

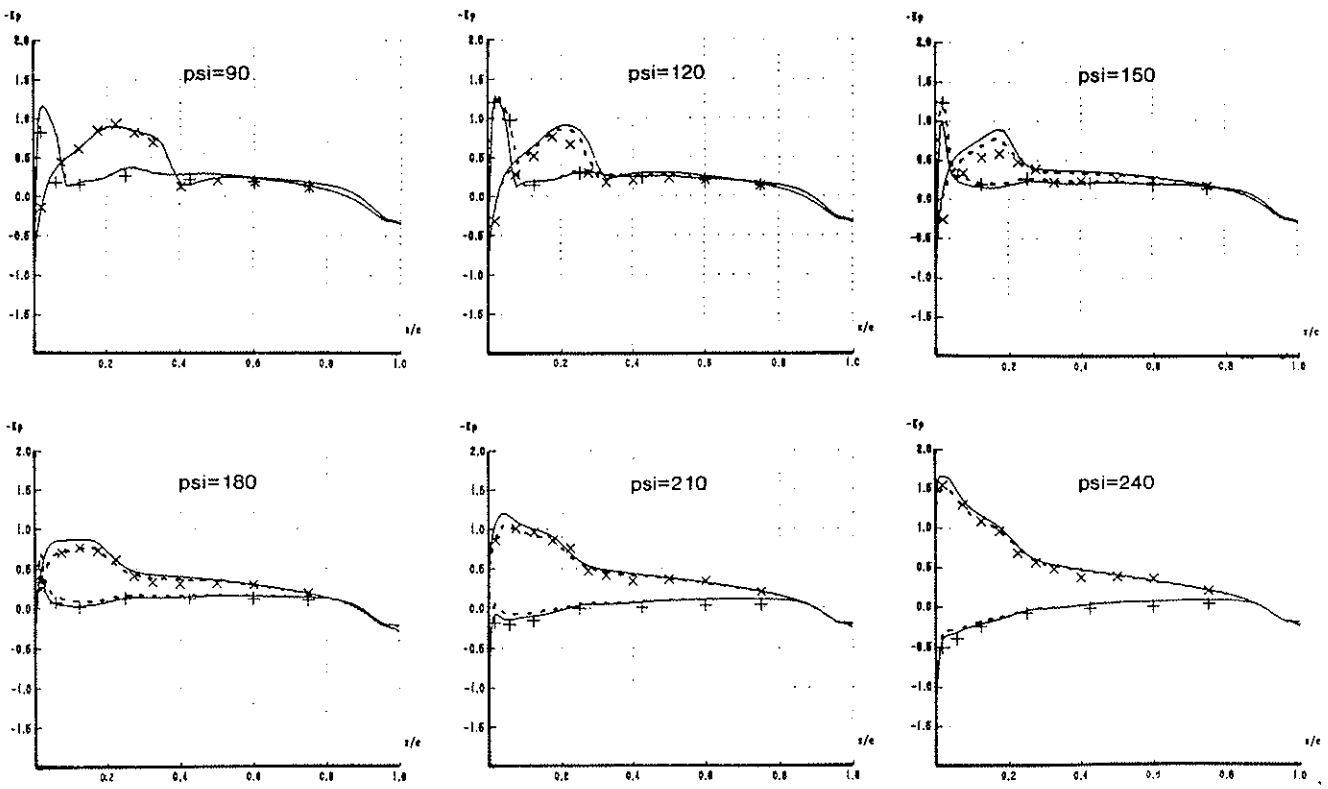


Fig.15 : r/R = 0.975